Dalton Transactions

Accepted Manuscript

ROYAL SOCIETY OF CHEMISTRY

www.rsc.org/dalton

Journal Name

ARTICLE

Thallophilic Tl(I)–Tl(I) Contacts Mediated by Tl–Aryl Interactions. A Computational Study.

Received 00th January 20xx,
Accepted 00th January 20xx

DOI: 10.1039/x0xx00000x

www.rsc.org/

Laura Weston,[a] Barnaby T. Pownall,[a] Francis S. Mair[a] and Joseph J. W. McDouall[a]

A computational study is presented of a complex of thallium with a neutral β-triketimine ligand which was found to form dimers with close Tl-Tl interactions. Single point energies, using the crystallographic structures, suggest that the system is bound only when BArF counter ions are included in the calculations. Energy decomposition analysis of the system was carried out in order to investigate the nature of the bonding. Across the methods, calculations show the electrostatic interaction to be repulsive for the dimer with no counter ions, but attractive when BArF counter ions are included. This suggests the metallophilic interaction is counter ion-mediated, requiring the anions to provide favourable electrostatics, even in the case of spatially diffuse and distant counter ions such as the 3,5-bistrifluoromethylphenyl borate ions used here.

Introduction

Metallophilic interactions are defined as weak metal-metal bonds occurring between pairs of atoms with the same formal charge. These very close interactions between metals were initially observed in complexes of gold, leading to the term aurophilicity.[1] Au–Au binding interactions have been shown to be in the range of 25-50 kJ mol^{-1} with corresponding Au–Au distances in the region of 2.8-3.5 Å.[2] These distances can be compared with twice the van der Waals and covalent radii of Au, which are 3.32 Å and 2.88 Å, respectively.

Such metal-metal interactions have since been observed between other metals, leading to the broader term metallophilicity, although examples involving Au show the strongest bonds. These metal-metal attractions are thought to be due to electron correlation, enhanced by relativistic effects.[3] The relevant electron correlation effects are dispersion and ionic electron exchange. The familiar dispersion interaction comes about through the instantaneous mutual polarisation of the electron clouds of two juxtaposed molecular units, while the ionic electron exchange interaction is an instantaneous charge-transfer between units.[4] These effects are enhanced by the relativistic contraction of 6s and 6p orbitals accompanied by expansion of 5d and 5f orbitals. Calculations on systems with aurophilic bonds suggest that these relativistic effects provide at least 15% of the aurophilic attraction.[5]

Metallophilic bonds involving thallium atoms (thallophilic), one of which was the subject of a recent experimental study,[6] have been observed at distances between 3.4-3.8 Å.[7] In comparison, twice the van der Waals and covalent radii of Tl are 3.92 Å and 2.96 Å, respectively. Tl–Tl bonds are on the weaker end of the metallophilic scale. Most systems involving a Tl(I)–Tl(I) bond are supported by bridging ligands, which help to stabilise the thallium atoms by filling its coordination sphere with lone pairs. Additionally, thallophilic systems usually involve ligands with a negative charge to counterbalance the charge on the thallium. There are examples of complexes exhibiting close Tl–Tl contacts which either form without ligand bridges, for example β-diketiminates complexes,[8,9] or which form with neutral ligands.[10] The thallium complex of interest in this study, **1** (see Figure 1) has neutral β-triketimine ligands.

[a] School of Chemistry, The University of Manchester, Manchester M13 9PL, UK. See DOI: 10.1039/x0xx00000x

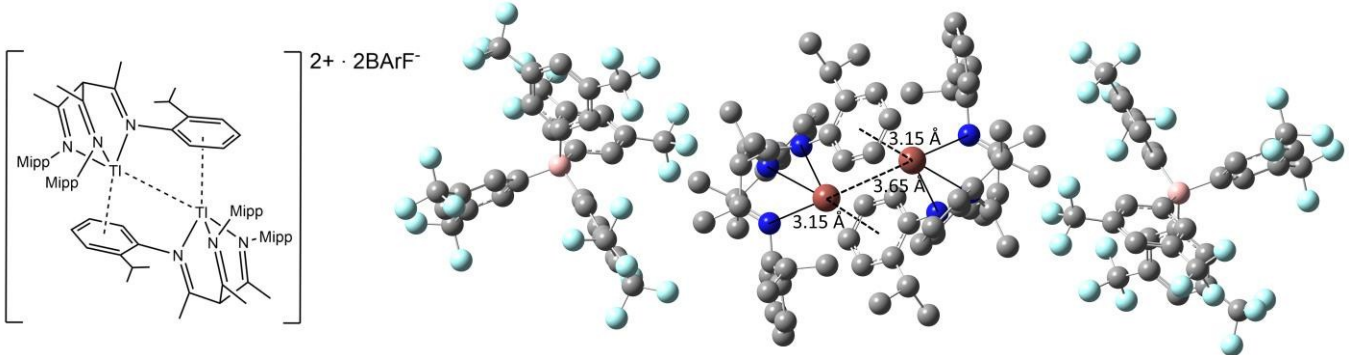

Figure 1 $[(tki^{Me3iPr3}Tl)_2]^{2+}2[BArF]^-$. Mipp=2-Pr^{i}C$_6H_4$

The complex: $tki^{Me3iPr3}Tl$ (β-triketimine = tki; the substituents on the imine carbon atoms are indicated, followed by an indication of the N-aryl substituents, which in all cases are *ortho*, hence $tki^{Me3iPr3}$ = HC{MeCN(2-iPrC6H5)3}) with BArF counter ions, where BArF=$[\{3,5\text{-}(CF_3)_2C_6H_3\}_4B]^-$ has been found to form dimers with Tl–Tl distances of 3.65 Å in the crystal geometry[6] (Figure 1). The $[(tki^{Me3iPr3Tl})_2]\cdot[BArF]_2$ system is an interesting case as the β-triketimine ligands are neutral, meaning the dimer without counter ions has a charge of 2+. The dimer also forms without ligand bridging taking place, unlike most thallophilic systems.

In the original experimental report it was suggested that the complex is held together despite unfavourable electrostatics due to aryl–Tl and Tl–Tl interactions as well as packing forces. Preliminary computations, using the crystal geometry, employed Hartree-Fock and density functional theory (DFT) methods but failed to predict any binding in the dimer structure. This was suggested to point to a problem with the representation of the necessary correlation effects in the methods employed. Though other workers have hinted at the importance of pairwise cation-anion (*i.e.* + + – –) interactions in explaining such dicationic structures.[11] It was originally supposed that the large metal-anion distances and the diffuse nature of the very large BArF anion meant that these effects could be ignored in seeking an understanding of the association, since the examples proven to rely on pairwise electrostatic effects employed much smaller and more charge-dense anions at shorter cation-anion distances. However in this work we show that such pairwise effects are essential in explaining the dimerisation of the cations, notwithstanding their distant diffuse nature. In the current study we develop the computational description of this intriguing system further by studying the interaction energy of the Tl(I) pairs in **1**, with and without the presence of counter ions. We also look at an energy decomposition analysis (EDA) to better understand the different components of the interaction energy. We begin by using a model system with Tl(I)–Tl(I) interactions, the Tl–H dimer, to assess the applicability of some *ab initio* and density functional methods to these types of interaction.

Computational Method

Calculations employed the Def2-SVP and Def2-TZVP basis sets.[12,13]. For the Tl atom, 60 core electrons were treated with a relativistic effective core potential[14] and the remaining 21 valence electrons with the corresponding Def2-SVP (4s4p2d) valence basis set.[15] The studies on **1** consist of single point calculations using the crystal structure.[6] *Ab initio* calculations on the model system were performed at the CCSD(T)[16], BD[17], MP2[18] and SCS-MP2[19] levels. In all wavefunction calculations reported here, all 21 valence electrons of the Tl atoms were correlated. For the purpose of EDA and the calculation of partial charges, within the natural population analysis (NPA) formalism[20], density functional calculations were carried out using the B97[21]-D3, B3LYP[22,23]-D3, M06-2X,[24] PBE[25,26]-D3 and PBE0[27]-D3 exchange-correlation functionals. Since most exchange-correlation functionals do not account for dispersion interactions to any significant extent, the widely used empirical D3 method developed by Grimme *et al*.[28] (with Becke-Johnson damping) was used in conjunction with the standard functionals: B97, B3LYP, PBE and PBE0. The M06-2X functional was also used, since it has shown considerable success in describing non-covalent interactions. Counterpoise corrections[29] were applied to all calculations of binding energies, except when discussing the EDA.

The EDA we have employed is that of Ziegler and Rauk,[30] using an in-house implementation. The binding energy (of a supermolecule composed of two fragments **A** and **B**) is decomposed into two parts as the fragments **A** and **B** come together to form **AB**:

$$\Delta E_{Bind}=\Delta E_{Prep}+\Delta E_{Int}$$

The preparation energy (ΔE_{Prep}) is the energy required to bring the two fragments, at their separated optimal geometries, together to form the supermolecule at its optimum geometry. The interaction energy (ΔE_{Int}) is further decomposed into four terms:

$$\Delta E_{Int}=\Delta E_{Elstat}+\Delta E_{Pauli}+\Delta E_{Orbital}+\Delta E_{Disp}$$

where ΔE_{Elstat} describes the interaction between the electrons of **A** with the nuclei of fragment **B** and vice versa. $\Delta E_{Orbital}$ arises from the orbital relaxation that takes place when the orbitals of the fragments (appropriately antisymmetrised and orthogonalised) rearrange to form the optimal orbitals of the supermolecule. The stabilising effects that form $\Delta E_{Orbital}$ include charge-transfer, polarization and other orbital mixing interactions. ΔE_{Pauli} arises from the repulsion of the electron clouds of the two fragments. The dispersion term, ΔE_{Disp}, was not included in the original formulation of Ziegler and Rauk. In this study ΔE_{Disp} is accounted for with the D3 model of Grimme.[15] Only ΔE_{Int} and its components are explored in this study since we have used the crystal geometry of **1** throughout and have made no attempt to optimise the geometry.

All calculations were carried out using the Gaussian 09 package.[31]

Results and Discussion

$(Tl–H)_2$

We wish to assess the physical factors responsible for the formation of **1**. To gauge the performance of the computational methods we use, we have studied the model system, Tl–H dimer. Schwerdtfeger[32] performed studies on this system using a variety of wavefunction-based methods and concluded that the Tl–H dimer should be observable at low temperatures using matrix isolation techniques. This system and has also been studied in the context of In…In and Tl…Tl metallophilic interactions in reference 33. Using the QCISD(T) method, Schwerdtfeger found a ground state singlet structure of C_{2h} symmetry with an optimal H–Tl–Tl angle of 115.1°, a Tl–Tl distance of 3.28 Å and a Tl–H distance of 1.894 Å, the corresponding binding energy being 14 kJ mol^{-1}. There is no indication in reference 32 that counterpoise corrections were

	Tl–H	$(Tl–H)_2$
R(Tl–H) / Å	1.9041 (1.87)[a]	1.8632
R(Tl–Tl) / Å		3.1914
ϑ(H–Tl–Tl) / °		120.54
ν_1 / cm^{-1}	1364.5	11.9
ν_2 / cm^{-1}		54.6
ν_3 / cm^{-1}		140.9
ν_4 / cm^{-1}		350.1
ν_5 / cm^{-1}		1410.5
ν_6 / cm^{-1}		1429.1
Zero-point energy / kJ mol^{-1}	8.1	20.3

Table 1 CCSD(T)/Def2-SVP optimised structure and properties of Tl–H and its dimer.
[a] Experimental value given in parentheses from K.P. Huber and G.Herzberg in *Molecular Spectra and Molecular Structure. IV. Constants of Diatomic Molecules,* Van Nostrand Reinhold, New York, 1979.

applied, so this binding energy is probably overestimated due to basis set superposition errors. An estimate of the difference in zero-point vibrational energies of only 5 kJ mol^{-1} led Schwerdtfeger to conclude that the Tl–H dimer should remain bound at low temperatures.

The optimised structures of Tl–H and the Tl–H dimer, obtained at the CCSD(T)/Def2-SVP level, are given in Table 1. The harmonic vibrational frequencies are also given, establishing the dimer structure as a minimum on the potential energy surface. The difference in zero-point energies of 4.1 kJ mol^{-1} is in close agreement with Schwerdtfeger's value.

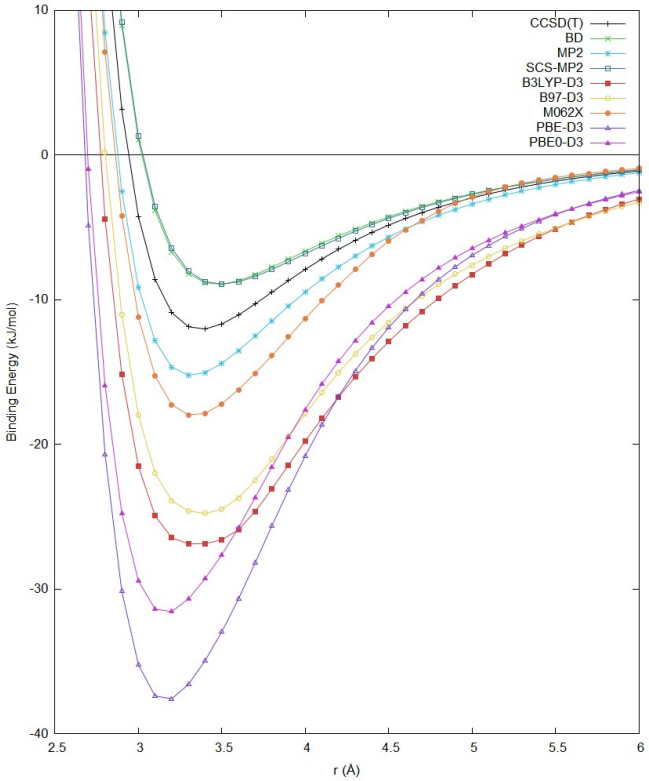

Figure 2 Binding energy of TlH dimer as a function of Tl-Tl distance (r) at various levels of theory using Def2-SVP basis set.

Method	R_{min} / Å	E_{bind} / kJ mol^{-1}
CCSD(T)	3.38	-12.1
BD	3.48	-9.1
MP2	3.33	-15.3
SCS-MP2	3.50	-9.1
B3LYP-D3	3.36	-26.9
B97-D3	3.39	-24.8
M06-2X	3.33	-17.9
PBE-D3	3.16	-37.8
PBE0-D3	3.16	-31.5

Table 2 Optimal value of Tl-Tl distance (R_{min}) and the corresponding binding energy (E_{bind}) at various levels of theory using Def2-SVP basis set. See Figure 2.

The Tl–H distance and the H–Tl–Tl angle were fixed at the CCSD(T) optimised values and the Tl–Tl distance was varied to produce the potential energy curves (including counterpoise correction) shown in Figure 2.

An important observation is that the C_{2h} structures optimised with the CCSD(T), BD and MP2 methods yield minima on the potential energy surface. A similar calculation at the CCSD level yields a saddle point, which if followed "downhill" yields a structure with unequal Tl–H distances. Using the density functional methods: PBE-D3 and PBE0-D3 a minimum structure is obtained. However, the B3LYP-D3, B97-D3 and M06-2X functionals yield saddle points. We re-optimised at the B3LYP and B97 levels to check whether the problem was with the D3 correction but also found saddle points at these levels, suggesting that the problem is associated with the functional. Interestingly, of the density functional methods tested, M06-2X despite predicting a saddle point, shows the closest alignment with the CCSD(T) curve. The binding energies and equilibrium distances for each method are given in Table 2.

All the DFT methods show very significant overestimation of the binding interaction. The MP2 method also overestimates the binding, while the SCS-MP2 method underestimates it. The BD potential energy curve is almost indistinguishable from the SCS-MP2 curve. The average of the MP2 and SCS-MP2 results appear to reproduce the CCSD(T) results quite well. These results are in accord with previous studies on coinage metal systems[34] that indicate the MP2 method overestimates metallophilic interactions in comparison with the higher CCSD and CCSD(T) levels.

Table 3 shows the EDA obtained using the PBE-D3, PBE0-D3 and M06-2X methods. The interaction energies shown differ

	PBE-D3	PBE0-D3	M06-2X
$\Delta E_{Orbital}$	-84.0	-76.9	-41.5
ΔE_{Elstat}	-97.7	-98.3	-66.8
ΔE_{Pauli}	146.1	146.9	89.6
ΔE_{Disp}	-2.9	-3.4	
ΔE_{Int}	-38.6	-32.3	-18.7

Table 3 Energy Decomposition Analysis on Tl-H dimer. All quantities are in kJ mol^{-1}.

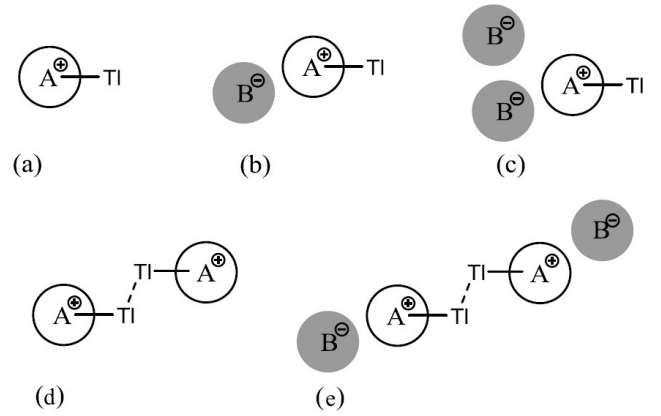

Figure 3 (a) (tki^{Me3iPr3})Tl) `Monomer' (b) [(tki$^{Me3iPr3}$)Tl)]·[BArF] `Monomer w. BArF' (c) [(tki^{Me3iPr3})Tl)]·[BArF]$_2$ `Monomer w. 2 BArF' (d) [(tki$^{Me3iPr3}$)Tl)$_2$] `dimer' (e) [(tki^{Me3iPr3})Tl)$_2$] · [BArF]$_2$ `Dimer w. BArF'.

from those in Table 2 since the EDA are carried out without counterpoise corrections. One immediately notices that ΔE_{Disp} provides only about 3 – 4 kJ mol^{-1} of binding, amounting to a small fraction (8 – 14%) of the binding energy. Certainly at the DFT level, the contribution of ΔE_{Elstat} and $\Delta E_{Orbital}$ appear more important. If we compare a dispersion energy of 4 kJ mol^{-1} with the binding energy at the CCSD(T) level, the contribution rises to about 34%. While this is a significant fraction, it still does not provide the dominant component of the binding energy.

It is instructive to compare the EDA based on the PBE and PBE0 functionals (the latter containing 25% Hartree-Fock exchange). The difference in the binding energy of 6.3 kJ mol^{-1} appears to come principally from $\Delta E_{Orbital,}$ with all the other terms each contributing less than 1 kJ mol^{-1} to the difference. From this model study we conclude that the MP2 and SCS-MP2 methods appear to bracket the CCSD(T) results, in the sense that the MP2 method overestimates the attractive interactions while the SCS-MP2 underestimates them. The average of the MP2 and SCS-MP2 interaction energies closely reproduce the interaction at the CCSD(T) level. All the DFT methods predict the Tl–H dimer to be significantly overbound. The DFT-based EDA imply that the dispersion energy is significant and important to the binding but is not the principal component.

Method	(tki^{Me3iPr3}Tl)$_2$	[(tki^{Me3iPr3}Tl)$_2$][BArf]$_2$
MP2	71.1	-53.1
SCS-MP2	60.1	-17.5
B3LYP-D3	16.9	-106.1
B97-D3	20.7	-103.0
M06-2X	69.5	-47.5
PBE-D3	38.3	-85.2
PBE0-D3	29.9	-92.5

Table 4 ΔEint (kJ mol^{-1}) corresponding to units (tki^{Me3iPr3}Tl)$_2$ and [(tki^{Me3iPr3}Tl)$_2$] · [BArF]$_2$, see Figure 3(d) and 3(e).

	No. of (tki^{Me3iPr3}Tl) units	No. of [BArF] units	B3LYP	M06-2X	PBE0
3(a)	1	0	0.823	0.867	0.837
3(b)	1	1	0.813	0.859	0.828
3(c)	1	2	0.809	0.856	0.824
3(d)	2	0	0.732	0.761	0.743
3(e)	2	2	0.730	0.760	0.740

Table 5 Charges on Tl atoms obtained from natural population analysis, corresponding to systems, as seen in Figure 3.

[(tki^{Me3iPr3}Tl)$_2$][BArf]$_2$ (1)

Several calculations were performed on the (tki^{Me3iPr3}Tl) system to assess the nature of the Tl–Tl interaction. A number of fragments have been used to investigate the complex, these are obtained from the crystal structure and are shown in Figure 3.

Counterpoise corrected single point calculations were carried out on the dimer and dimer with BArF counter ions (systems (d) and (e) from Figure 3). MP2 calculations were carried out with the Def2-SVP basis set, in all other cases the Def2-SVP basis set is used for the calculations with BArF counter ions and the Def2-TZVP basis set is used for the calculations without BArF counter ions. For the system without counter ions the basis set superposition error is approximately 0.037 au, illustrating the importance of counterpoise correction since the Def2-SVP basis set is far from complete for this large system. The resulting interaction energies are given in Table 4.

In all cases in which the [BArF]$^-$ ions were not included, the interaction energy between the (tki^{Me3iPr3}Tl) monomers was found to be repulsive. The MP2 and SCS-MP2 method both predict large positive (repulsive) interaction energies and while

Method	$\Delta E_{Orbital}$	ΔE_{Elstat}	ΔE_{Pauli}	ΔE_{Disp}	ΔE_{Int}
PBE-D3	-96.4	74.3	143.7	-108.0	13.5
PBE0-D3	-85.9	75.1	132.2	-111.5	9.8
B3LYP-D3	-88.3	73.7	175.4	-167.5	-6.7
B97-D3	-89.3	79.6	190.8	-184.2	-3.1
M06-2X	-82.8	70.5	66.4		54.1

Table 6 Energy Decomposition Analysis of (tki^{Me3iPr3}Tl)$_2$ ***without*** [BArF] counter ions. All quantities given in kJ mol^{-1}.

Method	$\Delta E_{Orbital}$	ΔE_{Elstat}	ΔE_{Pauli}	ΔE_{Disp}	ΔE_{Int}
PBE-D3	-88.5	-61.7	147.6	-109.2	-111.8
PBE0-D3	-78.3	-59.5	135.6	-112.7	-114.9
B3LYP-D3	-80.9	-61.7	179.7	-168.8	-131.8
B97-D3	-82.0	-56.0	195.2	-185.5	-128.3
M06-2X	-74.7	-63.9	68.9		-69.7

Table 7 Energy Decomposition Analysis of (tki^{Me3iPr3}Tl)$_2$·[BArF]$_2$ counter ions. All quantities given in kJ mol^{-1}.

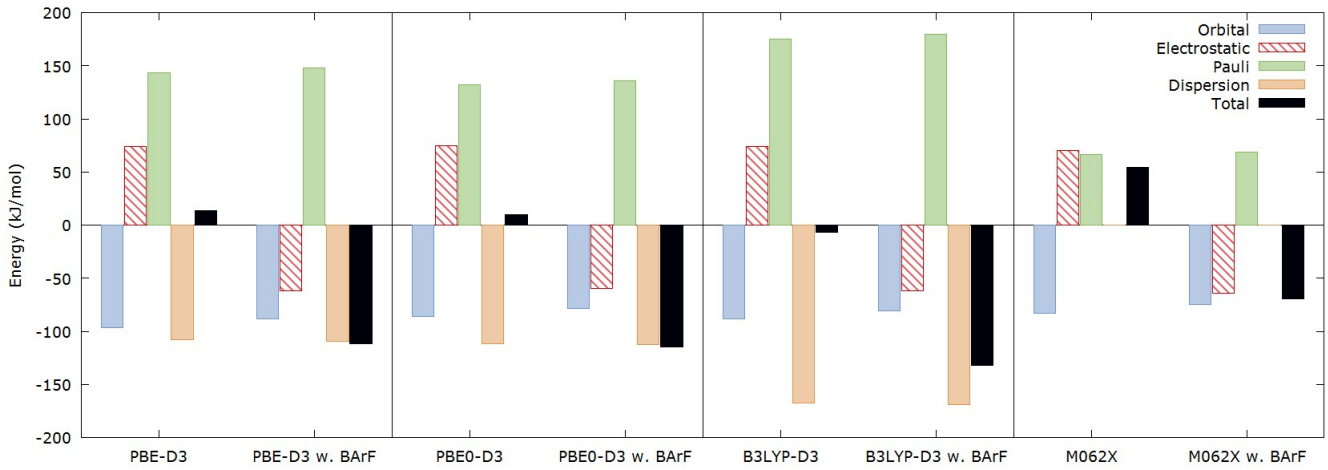

Figure 4 Orbital, electrostatic, Pauli and dispersion energy contributions to the total interaction energy of $(tki^{Me3iPr3}Tl)_2$ both with and without [BArF] counter ions, across a range of methods.

the DFT values are smaller, echoing the results on the model system, they still predict no binding.

The interaction energy for the system with counter ions included ($[(tki^{Me3iPr3}Tl)_2][BArF]_2$) was found to be attractive at all levels of theory. The largest binding energies were given by the B3LYP-D3, and B97-D3 methods. The M06-2X functional predicts a significantly smaller interaction energy than all the other DFT methods, with a value close to that obtained at the MP2 level. However, all methods are in qualitative agreement, *i.e.* that the system is bound. This gives some support to the idea of a counter ion-mediated interaction, in which the presence of the $[BArF]^-$ anions are required to balance the charge of the overall system and make the electrostatic interaction favourable.

To further investigate whether counter ion-mediated bonding is significant in this system, the NPA charge centred on the thallium atom in the ($tki^{Me3iPr3}Tl$) unit was calculated at the B3LYP, M06-2X and PBE0 levels using the Def2-SVP basis set in every combination shown in Figure 3. The results are shown in Table 5.

The PBE0 charges are in between those obtained at the B3LYP and M06-2X levels. The charge on Tl does decrease as the number of anion units is increased. However, this decrease is proportionately very small and not sufficient to explain the formation of a dimer. Comparison of the charge on Tl in ($tki^{Me3iPr3}Tl$) [BArF] with that in $(tki^{Me3iPr3}Tl)_2[BArF]_2$ shows that there is a larger decrease in charge when considering the system as a dimer than the difference made by the addition of counter ions alone. It is likely, then, that the inclusion of the counter ions must have a more subtle effect on the system than simply decreasing the charge on the Tl atoms.

Energy Decomposition Analysis calculations were run at a variety of DFT levels using the Def2-SVP basis to investigate the nature of the bonding and to shed light onto the effect that the $[BArF]^-$ counter ions have on the system. The results are shown in Figure 4 and Tables 6 and 7.

The interaction energies shown in Tables 6 and 7 differ from those in Table 4 since the EDA are carried out without counterpoise corrections, hence the B3LYP-D3 and B97-D3 methods predict a slightly bound system (with binding energies of –6.73 kJ mol^{-1} and –3.07 kJ mol^{-1} respectively) in the absence of counter ions. Inspection of Table 8 and Figure 4 shows that for all methods ΔE_{Elstat} is repulsive for the system without counter ions and becomes attractive once counter ions are included. This is by far the largest effect of the inclusion of counter ions and changes the interaction from repulsive to attractive. For all methods there is a decrease in the magnitude of $\Delta E_{Orbital}$ and an increase in that of ΔE_{Pauli} when counter ions are included, although these changes are small compared to the change in ΔE_{Elstat}. The addition of counter ions has a fairly small effect on ΔE_{Disp} and cannot be said to be the key factor in the binding of these units.

The importance of the ΔE_{Elstat} can be visualised by inspection of the electrostatic potential map in the region of the ($tki^{Me3iPr3}Tl$) with and without the counter ions. This is shown at the M06-2X/Def2-SVP level in Figure 5. The Tl atoms, as well as the ligands, are less positive in the system when counter ions are included. This suggests the effect of the counter ions is a broad one, lowering the charge across the thallium as well as the ligands. This allows the interaction between one Tl atom and the opposite ligand to overcome the Tl–Tl repulsion.

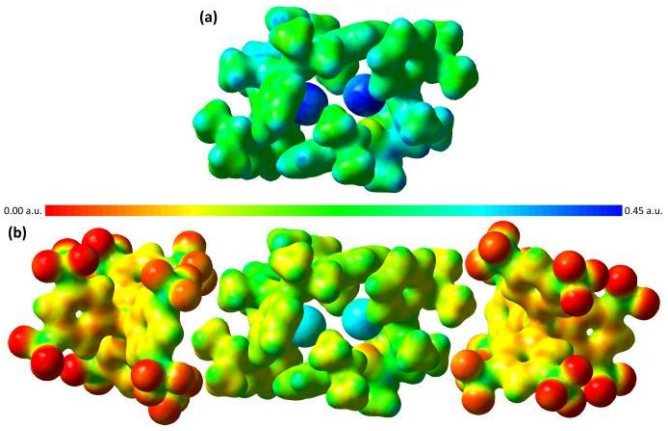

Figure 5 Electrostatic Potential Map of $[(tki^{Me3iPr3}Tl)]_2$ mapped onto a density surface with an isosurface value of 0.035 a.u. A) without and B) with [BArF] counter ions.

Although it should be borne in mind that these findings are based on a decomposition of the interaction energy between only two {(tki^{Me3iPr3}Tl)[BArF]} units. It is currently beyond our computational ability to assess the electrostatic influence of the full Madelung potential of the crystal.

The principal finding that the cation association is anion-mediated concurs with the analysis by Carvajal *et al*.[11] of $(L–Au)_2^{2+}$ dimers. However, it is distinguished from these prior findings by two points. Firstly, this is the first indication that a similar mechanism operates to bind $L–Tl^+$ cations into dimers. Secondly, all prior cases involved much smaller, more tightly bound anions, e.g. Cl^- (3.40 Å), Br^- (3.54 Å), $[BF_4]^-$ (3.67 Å) and $[PF_6]^-$ (3.93 Å) in comparison to the results herein. These show that the effect persists even when the cation-anion contacts extend to 5.9 Å and the negative charge is spread over 69 atoms, producing a much reduced charge density.

Conclusions

Our calculations have found evidence to partially support the suggestion by Mair[6] that aryl–Tl and Tl–Tl interactions hold the $[(tki^{Me3iPr3}Tl)_2][BArF]_2$ system together. There is strong support for the notion of a counter ion-mediated interaction. EDA and ESP results suggest that in the absence of counter ions the interaction energy is repulsive, but becomes attractive in the presence of the counter ions. The charge concentrated on the Tl atoms decreased with the addition of counter ion units, but only decreased significantly on the consideration of the system as a dimer. This suggests that the aryl–Tl interaction is key in holding the system together. ESP maps suggest that the presence of the counter ions has a broad effect across the Tl atoms as well as the ligands of (tki^{Me3iPr3}Tl) and it is this that enables the system to bind. By contrast the magnitude of the dispersion interaction appears not to be greatly affected by the presence of the counter ions.

Acknowledgements

L.W. thanks the School of Chemistry, The University of Manchester, for the award of a PhD studentship and Merck Chemicals Ltd for financial support.

Notes and references

1 F. Scherbaum, A. Grohmann, B. Huber, C. Krüger and H. Schmidbaur, *Angew. Chem. Int. Ed. Engl.* 1988, **27,** 1544.
2 H. Schmidbaur and A. Schier, *Chem. Soc. Rev*., 2008, **37** 1931.
3 P. Pyykkö and Y. Zhao, Angew. *Chem. Int. Ed. Engl*., 1991, **30**, 604.
4 S. Riedel, P. Pyykkö, R. A. Mata and H. J. Werner, *Chem. Phys. Lett*., 2005, **405,** 148.
5 P. Pyykkö, N. Runeberg and F. Mendizabal, *Chem. Eur. J*., 1997, **3,** 1451.
6 J. Cullinane, A. Jolleys and F. S. Mair,. *Dalton Trans*., 2013, **42,** 11971.
7 C. Janiak and R. Hoffmann, *J. Am. Chem. Soc*., 1990, **112,** 5924.
8 Y. Cheng, P. B. Hitchcock, M. F. Lappert and M. Zhou, *Chem. Commun*., 2005, 752.
9 M.S. Hill, R. Pongtavornpinyo and P.B. Hitchcock, *Chem. Commun*., 2006, 3720.
10 S. Welsch, C. Lescop, R. Réau and M. Scheer, *Dalton Trans*., 2009, 2683.
11 M. A. Carvajal, S. Alvarez and J. J. Novoa, *Theor. Chem. Acc*., 2006, **116**, 472.
12 K. Eickhorn, F. Weigend, O. Treutler and R. Ahlrichs, *Theor. Chem. Acc.*, 1997, **97**, 119.
13 F. Weigend, M. Häser, H. Patzelt and R.Ahlrichs, *Chem. Phys. Lett.*, 1998, **294**, 13.
14 B. Metz, M. Schweizer, H. Stoll, M. Dolg an W. Liu, *Theor. Chem. Acc.*, 2000, **104**, 22.
15 F. Weigend and R. Ahlrichs, *Phys. Chem. Chem. Phys.*,2005, **7**, 3297.
16 K. Raghavachari, G.W. Trucks, J.A. Pople and M. Head-Gordon, *Chem. Phys. Lett*., 1989, **157**, 479.
17 N.C. Handy, J.A. Pople, M. Head-Gordon, K. Raghavachari and G.W. Trucks, *Chem. Phys. Lett.*, 1989, **164**, 185.
18 M. Head-Gordon, J.A. Pople and M. J. Frisch, *Chem. Phys. Lett.*, 1988, **153**, 503.
19 S. Grimme, *J. Chem. Phys.*, 2003, **118**, 9095.
20 A.E. Reed, R.B. Weinstock and F. Weinhold, *J. Chem. Phys.*, 1985, **83**, 735.
21 A.D. Becke, *J. Chem. Phys.,* 1997, **107**, 8554.
22 A.D. Becke, *J. Chem. Phys*., 1993, **98,** 5648.
23 C. Lee, W. Yang, R.G. Parr, *Phys. Rev. B,* 1988, **37**, 785.
24 Y. Zhao and D. G. Truhlar, *Theor. Chem. Acc*., 2008, **120**, 215.
25 J. P. Perdew, K. Burke, and M. Ernzerhof, *Phys. Rev. Lett.,* 1996, **77,** 3865.
26 J. P. Perdew, K. Burke, and M. Ernzerhof, *Phys. Rev. Lett.,* 1997, **78**, 1396.
27 C. Adamo and V. Barone, *J. Chem. Phys.,* 1999, **110,** 6158.
28 S. Grimme, J. Antony, S. Ehrlich and H. Kreig*, J. Chem. Phys*., 2010, **132,** 154104.
29 S. F. Boys and F. Bernardi, *Mol. Phys*., 1970, **19,** 553.
30 T. Ziegler and A. Rauk, *Theoret. Chim. Acta*., 1977, **46**, 1.
31 Gaussian 09, Revision B.01, M. J. Frisch, G. W. Trucks, H. B. Schlegel, G. E. Scuseria, M. A. Robb, J. R. Cheeseman, G. Scalmani, V. Barone, B. Mennucci, G. A. Petersson, H. Nakatsuji, M. Caricato, X. Li, H. P. Hratchian, A. F. Izmaylov, J. Bloino, G. Zheng, J. L. Sonnenberg, M. Hada, M. Ehara, K. Toyota, R. Fukuda, J. Hasegawa, M. Ishida, T. Nakajima, Y. Honda, O. Kitao, H. Nakai, T. Vreven, J. A. Montgomery, Jr., J. E. Peralta, F. Ogliaro, M. Bearpark, J. J. Heyd, E. Brothers, K. N. Kudin, V. N. Staroverov, T. Keith, R. Kobayashi, J. Normand, K. Raghavachari, A. Rendell, J. C. Burant, S. S. Iyengar, J. Tomasi, M. Cossi, N. Rega, J. M. Millam, M. Klene, J. E. Knox, J. B. Cross, V. Bakken, C. Adamo, J. Jaramillo, R. Gomperts, R. E. Stratmann, O. Yazyev, A. J. Austin, R. Cammi, C. Pomelli, J. W. Ochterski, R. L. Martin, K. Morokuma, V. G. Zakrzewski, G. A. Voth, P. Salvador, J. J. Dannenberg, S. Dapprich, A. D. Daniels, O. Farkas, J. B. Foresman, J. V. Ortiz, J. Cioslowski, and D. J. Fox, Gaussian, Inc., Wallingford CT, 2010.
32 P. Schwerdtfeger, *Inorg. Chem*., 1991, **30,** 1660.
33 P. Pyykko, M. Straka and T. Tamm, *Phys. Chem. Chem. Phys.*, 1999, **1**, 3441.
34 E. O'Grady and N. Kaltsoyannis, *Phys. Chem. Chem. Phys*., 2004, **6**, 680.

Thallophilic interactions mediated by presence of coordinating anions provide 134 kJ mol^{-1} (M06-2X) electrostatic stabilisation.